Positional Response Characterization of 11 cm x 42.5 cm x 5.5 cm NaI(Tl) Detectors

Jordan Noey, Jeffery Xiao, Angela DiFulvio, Noor Sulieman, Marco Carmona, Issa El-Amir, Bhavin Gandhi,
Kevin Liu, Kai Schiefer, James Seekamp, Charles Sosa, David Trimas, Archan Vyas, Kimberlee Kearfott
Radiological Health Engineering Laboratory
Department of Nuclear Engineering and Radiological Sciences, University of Michigan, Ann Arbor, MI 48109-2104

Abstract

Experiments were performed with thirty 10.8 cm x 42.8 cm x 5.7 cm NaI:Tl detectors to better understand their positional response. Spectra were collected using 0.02 to 0.15 MBq point sources of Americium-241, Cesium-137, Cobalt-60, and Barium-133 positioned on parallel and perpendicular lines to the long axis of the crystal along both the narrow and wide detector faces as well as at different distances from them. A greater density of positions was sampled at the ends of the detector and repeated measurements were made to examine potential gain drifts during the course of the experiment. Spectroscopic peak counts, pulse heights, gross counts, and net counts were analyzed. Empirical equations were fit to those data for each specific source energy as a function of source position. In addition, a Monte Carlo radiation transport code was used to simulate the expected positionally-variable response based solely upon radiation absorption. The simulated radiation transport efficiency functions were compared to the experimental data. The effects of the geometric radiation efficiency, the attenuation and scattering of emitted light within the scintillation crystal, and nonuniformity of the photomultiplier tube (PMT) photocathode response were then distinguished. Functions describing each effect were derived. The results suggest potential new corrections to data used to locate photon absorption events using large scintillation detectors such as those employed for nuclear medicine imaging.

Methods

Experimental Setup and Materials

Equipment and source information table used during routine data collection along with the experimental setup with source position 18 cm from the PMT.

Equipment	*Model*
Ortec Integrated Electronics	MFG-digiBASE
Saint Gobain NaI Scintillator with Bicron Photomultiplier Tube	2X4H16/3.5A
Radionuclide	*Activity (MBq)* *
Cobalt-60 (i)	0.011
Cobalt-60 (ii)	0.015
Barium-133	0.036
Cesium-137	0.14
Americium-241	0.15

* *Activity at time of experimentation*

(a) Top view

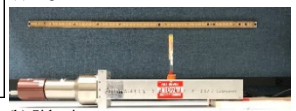

(b) Side view

Energy Spectrum

Typical spectrum of collected data with source peaks Americium-241 (1), Barium-133 (2), Cesium-137 (3), Cobalt-60(i) (4), and Cobalt-60 (ii) (5).

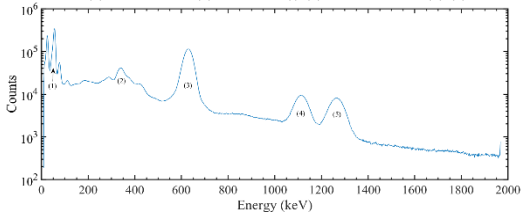

Results

Transverse Measurements

Measurements of photopeak net counts and photopeak channel number (a measure of pulse height) of Cesium-137 were collected across the photomultiplier tube (PMT) at four varying distances perpendicular to the long axis of the detector. Equations were fit to model the behavior of each of the collected quantities.

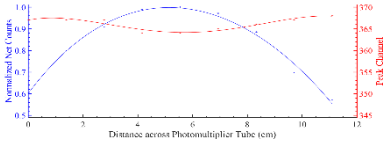

(a) Typical response curve of normal behaving detector with source position 0.64 cm from PMT. Functional fits: $\chi^2_{channel}$=0.95, χ^2_{counts}=0.98.

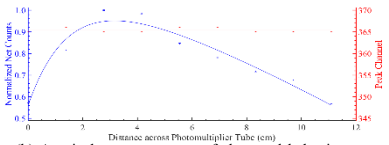

(b) Atypical response curve of abnormal behaving detector with source position 0.64 cm from PMT. Functional fits: $\chi^2_{channel}$=0.75, χ^2_{counts}=0.95.

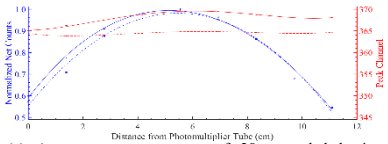

(c) Average response curve of 28 normal behaving detectors from 0.64 cm (solid) to 2.54 cm (dashed) from PMT. Functional fits (0.64 cm): $\chi^2_{channel}$=0.993, χ^2_{counts}=0.9997; (2.54 cm): $\chi^2_{channel}$=0.992, χ^2_{counts}=0.98.

Face Wide Center Measurements

Measurements of photopeak net counts and photopeak channel number (a measure of pulse height) of Cesium-137 were collected at varying distances perpendicular to the long axis of the detector. Equations were fit to model the behavior of each of the collected quantities.

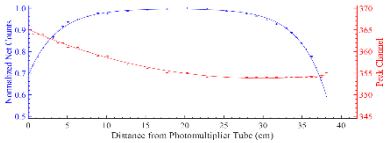

(a) Typical response curve of normal behaving detector with source position centered with respect to the PMT. Functional fits: $\chi^2_{channel}$=0.996, χ^2_{counts}=0.998.

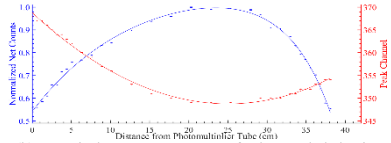

(b) Atypical response curve of abnormal behaving detector with source position centered with respect to the PMT. Functional fits: $\chi^2_{channel}$=0.995, χ^2_{counts}=0.98.

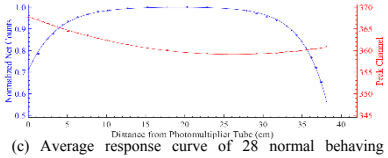

(c) Average response curve of 28 normal behaving detector with source position centered with respect to the PMT. Functional fits: $\chi^2_{channel}$=0.998, χ^2_{counts}=0.9998.

Empirical Functions

$$F(x) = a + [b(1 - e^{-cx})] + d(1 - fe^{x-g}) \quad (1)$$

Equation (1) models normalized net counts for face wide center and transverse measurements as a function of distance from the PMT with fitted parameters a, b, c, d, f, and g.

$$G(x) = ae^{-bx} + ce^{-dx} \quad (2)$$

Equation (2) models the peak channel for face wide center measurements and the simulated versus experimental difference as a function of distance from the PMT with fitted parameters a, b, c, and d.

$$H(x) = ax^4 + bx^3 + cx^2 + dx + f \quad (3)$$

Equation (3) models the peak channel for transverse measurements as a function of distance across the PMT with fitted parameters a, b, c, d, and f.

Fitted Parameters	Transverse Normalized Net Counts			
	Typical	Atypical	Average (Row 1)	Average (Row 4)
a	-0.7778	0.6198	0.3065	0.332
b	1.183	0.4329	0.275	0.995
c	0.5084	0.6472	0.1368	0.07369
d	0.1282	0.02685	0.07363	0.07532
f	1.318	1.812	1.668	0.753
g	16.59	2.581	2.527	16.51

Fitted Parameters	Transverse Peak Channel			
	Typical	Atypical	Average (Row 1)	Average (Row 4)
a	-0.00165	-	0.003631	0.002244
b	0.1349	-	-0.07986	0.05122
c	-0.8949	-	0.4388	0.3946
d	1.246	-	0.1701	0.8877
f	367.2	275.6	378.1	377.4

Fitted Parameters	Face Wide Center Normalized Net Counts		
	Typical	Atypical	Average
a	0.6886	-0.6196	0.4635
b	0.5181	0.9431	0.2958
c	0.2798	0.08341	0.2486
d	0.2678	0.2013	0.3181
f	1.358	0.001937	0.2449
g	45.61	-4.437	36.3

Fitted Parameters	Face Wide Center Peak Channel		
	Typical	Atypical	Average
a	119.7	2642	1514
b	-0.01525	0.01213	0.01227
c	2454	1046	2162
d	-0.004345	-0.01538	0.005445

Fitted Parameters	Simulated Minus Average Normalized Net Counts	
	Positions 1-16	Positions 17-32
a	0.6192	0.6618
b	0.3597	-0.3458
c	0.4951	-0.6267
d	0.4096	-0.4774
f	0.6915	-
g	21.86	-

Fitted parameters used for each graphical function shown above

Simulated Measurements

Photopeak net counts were collected along the front wide center face for Cesium-137 based only on radiation transport. The program used for simulation was MCNP.

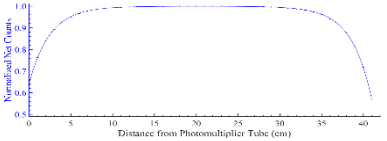

Simulated response curve of normal behaving detector. Functional fits: χ^2_{counts}=0.999998.

Simulated versus Experimental Data

Differences in radiation transport simulations and experimental data for Cesium-137 reveal the effects of light scattering and attenuation.

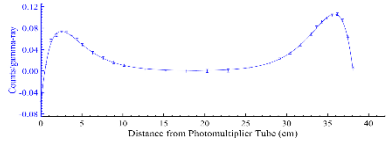

Difference of simulated minus average face wide center. Functional fits: χ^2_{counts}=0.9992.

Conclusion

Radiation transport simulations helped separate radiation from light scattering and attenuation effects in experimental data. A single parametric equation provided an excellent fit for sensitivity as a function of source position for 28 of 30 detectors tested. Pulse height varied measurably and consistently as a function of distance along the crystal axis because of light scatter at both ends of the crystal, light attenuation, and photocathode nonuniformity. Knowledge of these reproducible empirical equations enables improved estimation of overall system sensitivity and uniformity for various detector arrangements. With the precise knowledge of pulse height variations with position, corrections are possible resulting in improvements in the spectrum for large scintillators. Intentional enhancement of light attenuation to improve the effect could result in positional discrimination without physical or electronic collimation when the radionuclide is known.

Acknowledgements Special thanks are extended to Dr. Richard T. Kouzes, Laboratory Fellow at the Department of Energy's (DOE's) Pacific Northwest National Laboratory (PNNL), for the loan of the detectors. This work was funded by the Consortium for Verification Technology under the Department of Energy National Nuclear Security Administration, award number DE-NA0002534.